Uptake of nitrate and sulfate on dust aerosols during TRACE-P

C. E. Jordan,[1] J. E. Dibb,[2] B. E. Anderson,[1] and H. E. Fuelberg[3]

Received 30 October 2002; accepted 22 May 2003; published 24 September 2003.

[1] Aerosol data collected near Asia on the DC-8 aircraft platform during TRACE-P has been examined for evidence of uptake of NO_3^- and $SO_4^=$ on dust surfaces. Data is compared between a sector where dust was predominant and a sector where dust was less of an influence. Coincident with dust were higher mixing ratios of anthropogenic pollutants. HNO_3, SO_2, and CO were higher in the dust sector than the nondust sector by factors of 2.7, 6.2, and 1.5, respectively. The colocation of dust and pollution sources allowed for the uptake of NO_3^- and nss-$SO_4^=$ on the coarse dust aerosols, increasing the mixing ratios of these particulates by factors of 5.7 and 2.6 on average. There was sufficient nss-$SO_4^=$ to take up all of the NH_4^+ present, with enough excess nss-$SO_4^=$ to also react with dust $CaCO_3$. This suggests that the enhanced NO_3^- was not in fine mode NH_4NO_3. Particulate NO_3^- (p-NO_3^-) constituted 54% of the total NO_3^- (t-NO_3^-) on average, reaching a maximum of 72% in the dust sector. In the nondust sector, p-NO_3^- contributed 37% to t-NO_3^-, likely due to the abundance of sea salts there. In two other sectors where the influence of dust and sea salt were minimal, p-NO_3^- accounted for <15% of t-NO_3^-. *INDEX TERMS:* 0305 Atmospheric Composition and Structure: Aerosols and particles (0345, 4801); 0345 Atmospheric Composition and Structure: Pollution—urban and regional (0305); 0365 Atmospheric Composition and Structure: Troposphere—composition and chemistry; 0368 Atmospheric Composition and Structure: Troposphere—constituent transport and chemistry; *KEYWORDS:* heterogeneous uptake of nitrate, Asian dust, TRACE-P

Citation: Jordan, C. E., J. E. Dibb, B. E. Anderson, and H. E. Fuelberg, Uptake of nitrate and sulfate on dust aerosols during TRACE-P, *J. Geophys. Res.*, *108*(D21), 8817, doi:10.1029/2002JD003101, 2003.

1. Introduction

[2] The two primary objectives of NASA's Transport and Chemical Evolution over the Pacific (TRACE-P) mission were to characterize the sources and chemical composition of Asian outflow and to study the evolution of this outflow. As part of this mission, measurements of aerosol chemical and physical properties were made aboard the DC-8 aircraft [see *Jordan et al.*, 2003; *Dibb et al.*, 2003]. Samples clearly influenced by dust were obtained. Recent modeling and laboratory studies [e.g., *Zhang et al.*, 1994; *Dentener et al.*, 1996; *Xiao et al.*, 1997; *Goodman et al.*, 2000; *Phadnis and Carmichael*, 2000; *Song and Carmichael*, 2001a, 2001b; *Underwood et al.*, 2001] have suggested that alkaline dust particles can take up acids resulting in increased coarse mode NO_3^- and $SO_4^=$. In this paper, we report in situ evidence collected regionally aboard the DC-8 that supports prior indications that such uptake occurs in the atmosphere.

[3] Using 40 years of dust storm records, *Sun et al.* [2001] describe how dust is transported out of China. These dust storms occur predominantly in spring [*Liu*, 1985; *Sun et al.*, 2001] and are due to cold air outbreaks which cause frontal systems and the Mongolian cyclonic depression. About 78% of dust storms are associated with the Mongolian cyclone with the remainder associated solely with the passage of cold fronts [*Sun et al.*, 2001]. There are two dominant source regions of dust in East Asia, the gobi deserts in Mongolia and northern China, and the Taklimakan Desert in western China. Owing to the mountains surrounding the Taklimakan, dust can only be exported out of this region when strong easterlies loft dust above 5 km in altitude (the height of the mountains). At these heights, this dust becomes entrained in the jet stream and may then be transported long distances over the Pacific Ocean and to North America. Dust from the gobi deserts of Mongolia and northern China on the other hand, is generally lofted to altitudes <3 km and then transported in a southeasterly direction, depositing dust on the Loess Plateau, eastern Asia, and the western Pacific (Figure 1 [*Sun et al.*, 2001]).

[4] The mineralogy of loess at its source consists primarily of quartz (SiO_2), feldspars, micas, clays, carbonates (primarily $CaCO_3$), and several minor minerals [*Pye*, 1987; *Gao and Anderson*, 2001]. The carbonate content is relatively constant at 12% by weight in loess, dust, and ground surface samples [*Derbyshire et al.*, 1998]. *Nishikawa et al.* [1991] found that weight fractions of $SO_4^=$ in soils of arid regions of China ranged from <0.01% to 0.46%, insufficient to account for the high fraction of $SO_4^=$ in dust downwind

[1]NASA Langley Research Center, Hampton, Virginia, USA.
[2]Climate Change Research Center, Institute for the Study of Earth, Oceans, and Space, University of New Hampshire, Durham, New Hampshire, USA.
[3]Department of Meteorology, Florida State University, Tallahassee, Florida, USA.

0148-0227/03/2002JD003101$09.00

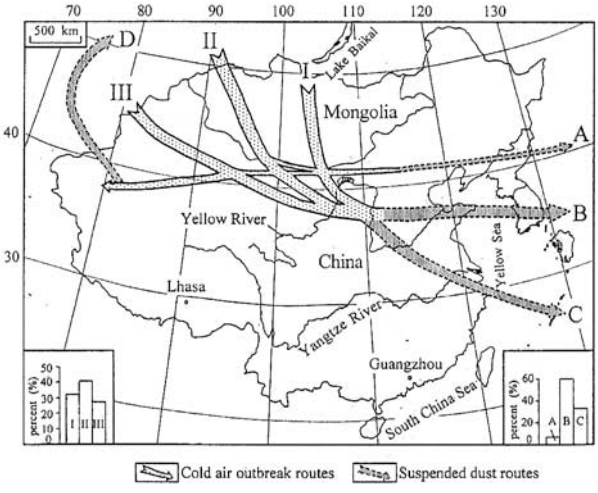

Figure 1. Map of cold air outbreaks and suspended dust routes in East Asia, from *Sun et al.* [2001].

of these regions. Individual dust particles from five dust storms in Beijing examined by *Zhang and Iwasaka* [1999] showed very little water-soluble $SO_4^=$ on the surface of these particles. Only ~15% of the particles had a sulfur peak; even fewer, 11%, showed any NO_3^-. This suggests that little chemical alteration takes place prior to reaching Beijing. Yet, samples collected in Qingdao, 500 km southeast of Beijing, showed 50–80% of the coarse particles (>2 μm diameter) were coated with $SO_4^=$ [*Parungo et al.*, 1995]. This chemical alteration then must occur downstream from Beijing.

[5] The presence of $CaCO_3$ in Asian dust is important because it reacts with acids such as sulfuric and nitric acid. In this way, dust particles may be chemically altered from their original composition at their source. Assuming the dust particles travel along a path where anthropogenic S and N sources are important, the surface area provided by the dust particles may lead to significant alteration of the air mass chemistry as SO_2 and HNO_3 transfer from gas to particulate phase [*Zhang et al.*, 1994; *Xiao et al.*, 1997; *Song and Carmichael*, 2001a, 2001b]. The presence of these acidic ions on dust can change the solubility of the aerosol from hydrophobic to hydrophilic [*Song and Carmichael*, 2001a].

[6] Evidence of $SO_4^=$ and NO_3^- on dust is found in studies of individual particles [e.g., *Wu and Okada*, 1994; *Parungo et al.*, 1995; *Gao and Anderson*, 2001] as well as studies of bulk aerosol composition [e.g., *Choi et al.*, 2001; *Kim and Park*, 2001] and precipitation [e.g., *Minoura et al.*, 1998]. Individual particles show both NO_3^- and $SO_4^=$ inclusions along with $CaCO_3$, as well as particles where all of the $CO_3^=$ has been replaced [*Wu and Okada*, 1994; *Parungo et al.*, 1995; *Gao and Anderson*, 2001]. Bulk aerosols from dust events show that the dominant water-soluble ions are $SO_4^=$, NO_3^-, Ca^{2+}, and Mg^{2+} [*Choi et al.*, 2001; *Kim and Park*, 2001]. Where size-resolved data is available, NO_3^- and $SO_4^=$ are found primarily in the coarse fraction associated with Ca^{2+} during dust events [*Kim and Park*, 2001]. In the absence of dust, $SO_4^=$ is primarily in the fine mode, while NO_3^- can be associated with either NH_4^+ in the fine mode [*Kim and Park*, 2001; *Song and Carmichael*, 2001a] or Na^+ in the coarse mode [*Song and Carmichael*, 2001a]. In precipitation in Japan the highest average concentrations of NO_3^-, $SO_4^=$, and Ca^{2+} are observed during Kosa (dust storm) events [*Minoura et al.*, 1998]. The low pH of precipitation during these dust events is attributed to the large amounts of acidic ions on the Kosa particles scavenged by the precipitation [*Minoura et al.*, 1998]. By the time dust particles reach Korea and Japan, ~75% of the carbonate has been displaced by $SO_4^=$ and NO_3^- [*Nishikawa et al.*, 1991].

[7] Various modeling studies have estimated the degree to which heterogeneous reactions contribute to the production of coarse mode $SO_4^=$ and NO_3^-. *Chameides and Stelson* [1992] estimated >70% of $SO_4^=$ formed by heterogeneous reactions. Using a regional three-dimensional (3-D) model for the period 1–14 March 1994, *Xiao et al.* [1997] estimated chemical conversion of SO_2 in the presence of dust contributed 20–40% to total $SO_4^=$ production in East Asia. *Song and Carmichael* [2001a], also using a regional 3-D model, found heterogeneous reactions account for 10–40% of $SO_4^=$ production in dust plumes and 10–80% in sea-salt-dominant regions. They attribute the greater production of $SO_4^=$ on sea salt versus dust to the dust mass distribution having a larger coarse fraction than sea salt.

[8] *Dentener et al.* [1996] looked at irreversible reactions of HNO_3, N_2O_5, NO_3, HO_2, O_3, and SO_y on dust surfaces. They predicted that a substantial fraction of $SO_4^=$ is associated with mineral aerosol. They also found that an even larger fraction of gas phase HNO_3 may be neutralized by mineral aerosol. *Phadnis and Carmichael* [2000] predict >70% of gas-phase HNO_3 is partitioned onto dust over the gobi deserts, while 10–70% of HNO_3 ends up in particulate phase over the rest of East Asia. *Song and Carmichael* [2001a] predict 10–50% of HNO_3 partitioned into NO_3^- in the boundary layer, with this partitioning exceeding 70% in dust and sea-salt plume centers. In the free troposphere, they predict 10–30% of HNO_3 partitioned into particulate phase, increasing to >50% in dust plume centers. *Song and Carmichael*'s model [2001a] also suggests that while NO_3^- resides primarily in coarse mode, in regions with abundant NH_3 and HNO_3, fine mode NH_4NO_3 may be found. The region where this is most likely to occur is around the lower Huang River, where there is high population density and agricultural activity [*Song and Carmichael*, 2001a].

[9] A laboratory study of the uptake of HNO_3 on $CaCO_3$ particles [*Goodman et al.*, 2000] found the reaction was limited to the particle surface in the absence of water. However, in the presence of water vapor the reaction was not limited to the surface of the particle. *Underwood et al.* [2001] studied the uptake of NO_2 and HNO_3 in the laboratory coupled with model calculations. They found that while uptake of NO_2 does not appear to be significant, uptake of HNO_3 is significant, with mixing ratios reduced by 30%. They note that this fraction is likely to increase under humid in situ conditions versus the dry conditions of their experiment.

[10] A companion paper [*Jordan et al.*, 2003] presents a thorough discussion of the DC-8 aerosol observations during TRACE-P in the context of four source regions based on back trajectories. These four sectors are NNW, Channel, WSW, and SE Asia (moving roughly counterclockwise from north to south). WSW and SE Asia samples were

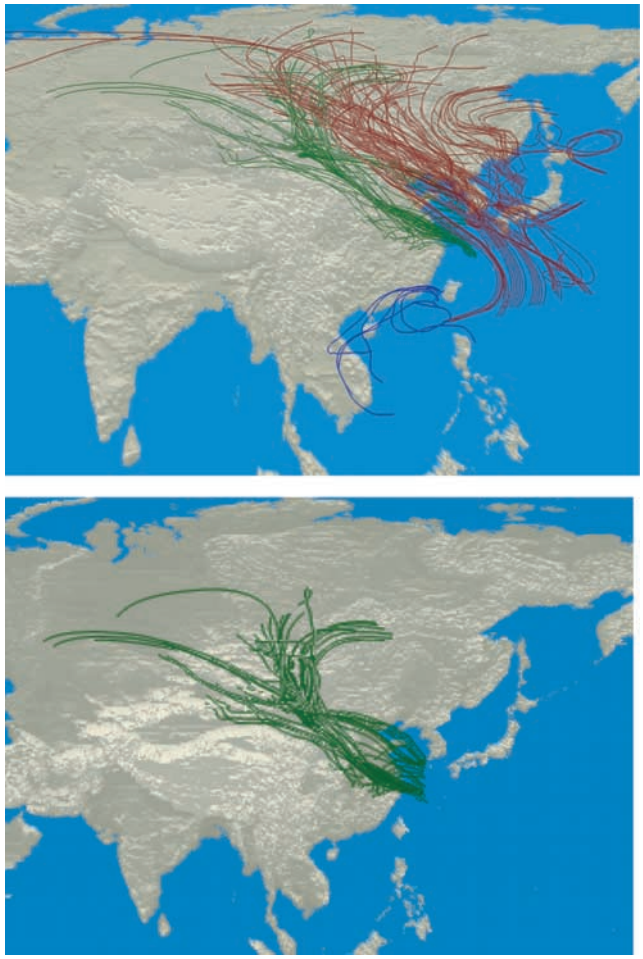

Figure 2. Back trajectories of the dust sector (Channel, green lines) and the nondust sector (NNW, red lines).

generally collected above 2 km altitude and represent relatively long range transport. NNW and Channel included many low altitude samples (<2 km) which were heavily influenced by sea salts (both sectors) and dust (Channel). Here we focus on these latter two sectors to look for evidence of gas to particle transfer of NO_3^- and $SO_4^=$.

2. Approach

[11] Back trajectories coupled with aerosol chemical data were used to classify the DC-8 TRACE-P aerosol data into four groups [*Jordan et al.*, 2003]. The back trajectories were calculated using a kinematic model based on global meteorological analyses from the European Centre for Medium-Range Weather Forecasts (ECMWF) [*Fuelberg et al.*, 2003]. The chemical samples were collected over periods ranging from ~5 to 35 min during level flight legs. The back trajectories were calculated every 5 min during level flight legs. Thus an individual aerosol sample might have anywhere from one to seven back trajectories associated with it. Samples that had multiple trajectories which emanated from more than one of the four sectors were classified as mixed and were not used any further in the analysis. The idea was to obtain a set of samples that represented a given sector with as little interference from other sectors as possible. In this way, 77 samples were obtained for the NNW sector, 38 for Channel, 31 for SE Asia, and 47 for WSW.

[12] NNW and Channel trajectories both emanate from northern Asia, with the Channel trajectories bounding the NNW trajectories to the south and west (Figure 2, top). The Channel trajectories themselves are bounded to the south by the Tibetan Plateau. WSW trajectories (not shown here) typically reflect high altitude, long range transport from the west as far away as Africa. SE Asia trajectories tend to circle over the western Pacific and southeast Asia. Both of these latter sectors have much lower mixing ratios of aerosols in general than the two former sectors, making them less appropriate for a comparison which tries to isolate the dust component. For a more extensive discussion of the sampling method and back trajectory calculations, please refer to the work of *Jordan et al.* [2003]. A complete discussion of the aerosol properties of each sector appears in that paper. Here the intention is to use just the Channel and NNW sectors to examine the influence of dust on aerosol chemistry, particularly, the uptake of NO_3^- and $SO_4^=$ on dust surfaces. Note that mixing ratios (pptv) were converted to moles or mass per unit volume using standard cubic meters rather than volumetric cubic meters (e.g., $\mu g\ m^{-3}$ STP or $\mu mol\ SCM^{-1}$).

3. Discussion

[13] *Sun et al.* [2001] described the pathways of the cold air outbreaks which lead to dust storms, as well as the pathways the suspended dust particles follow once suspended (Figure 1). Pathway I is followed by cold air masses near Lake Baikal which move southward across central Mongolia and China. Pathway II involves cold air masses in the northwest which result in dust storms along the Hexi Corridor (a northwest-southeast trending geographic region which connects the Xinjiang and Gansu provinces) and gobi deserts in northern China. Pathway III results in dust storms both in the Hexi Corridor and Taklimakan Desert. Most of the cold air outbreaks follow pathway II (41%), followed by pathway 3 (37%), and pathway I (32%). *Sun et al.* [2001] then break down the routes the suspended dust travels. Routes A, B, and C (Figure 1) carry dust from the gobi deserts in Mongolia and China depositing it en route to Korea, Japan, and the Pacific Ocean. Route B is most common (60%) followed by C (33%), then A (7%). Route D carries dust out of the Taklimakan Desert to high altitudes where it becomes entrained in the jet stream and is transported long distances downwind [*Sun et al.*, 2001].

[14] During TRACE-P, using aerosol chemistry coupled with back trajectories, we determined the path followed by the majority of the dust observed by the DC-8 [*Jordan et al.*, 2003]. The back trajectories for these dust samples (Figure 2, bottom) closely resemble the C and B routes described by *Sun et al.* [2001] (Figure 1).

[15] In order to investigate the role of dust in heterogeneous uptake of NO_3^- and $SO_4^=$, we compare the dust sector (Channel) to the adjacent sector (NNW). The primary distinction between these sectors is the presence of dust. However, Channel also has higher pollution inputs as well, as evidenced by gas phase species such as HNO_3 and CO (Table 1). This results in all aerosol species showing higher

Table 1. Means, Standard Deviations, Medians, Minima, Maxima, and Number of Samples for Various Aerosol and Gas Phase Species[a]

	NO_3^-, nmol/m^3	nss-$SO_4^=$, nmol/m^3	nss-Ca^{2+}, nmol/m^3	Na^+, nmol/m^3	NH_4^+, nmol/m^3	HNO_3, nmol/m^3	SO_2, nmol/m^3	CO, ppbv	Ethyne/CO, pptv/ppbv
				Channel					
Mean ± st. dev.	74 ± 110	91 ± 91	168 ± 177	64 ± 91	104 ± 115	44 ± 49	147 ± 173	258 ± 138	3.3 ± 1.1
Median (min.-max.)	40 (1–60)	78 (5–491)	115 (2–622)	26 (1–314)	92 (6–639)	33(6–264)	115(1–931)	256 (109–830)	3.2 (1.9–8.0)
No. of samples	38	38	38	38	38	38	33	38	38
				NNW					
Mean ± st. dev.	13 ± 16	35 ± 26	10 ± 12	57 ± 70	38 ± 29	17 ± 13	24 ± 36	176 ± 49	3.0 ± 0.8
Median (min.-max.)	6 (1–90)	31 (3–96)	5 (0–59)	12 (1–255)	26 (1–101)	17(3–61)	8(1–174)	185 (43–266)	3.1 (0.9–4.6)
No. of samples	77	77	77	77	77	76	62	77	75

[a]St. dev., standard deviation; min., minimum; max., maximum; no., number.

means in Channel than NNW except for Na^+. The primary source of Na^+ in the DC-8 measurements is sea salt; hence there is little difference between the mean mixing ratios for these groups.

[16] As discussed by *Keene et al.* [1986], Na^+ and Mg^{2+} are generally considered the best tracers of sea salt. However, this can become complicated when crustal sources add a significant amount to these species in coastal environments. Comparing the measured ratio of Mg^{2+}/Na^+ to the equivalence ratio of 0.227 found in bulk seawater [*Wilson*, 1975; *Keene et al.*, 1986], one can determine which species to use as the reference sea-salt species. A ratio in excess of 0.227 indicates a crustal Mg^{2+} influence, while a ratio less than this suggests a crustal Na^+ component. Here the data closely adheres to the sea-salt ratio for the NNW group (Figure 3). However, Mg^{2+} is clearly enhanced in Channel, altering the slope significantly from what one would expect for sea salt (Figure 3). Thus for this study, Na^+ is used as the reference species for sea salt, since it appears less likely to suffer from major deviations from the marine source. However, it is known that Na^+ is a component of Asian dust [*Song and Carmichael*, 2001b]. Hence in calculating the sea-salt and non-sea-salt components of the aerosol species reported here, the sea-salt component will be somewhat overestimated, leading to an underestimate of non-sea-salt species for the Channel group.

[17] The distribution of NO_3^-, HNO_3, nss-Ca^{2+}, Na^+, nss-$SO_4^=$, and NH_4^+ as a function of altitude show that most species are enhanced at low altitudes (Figure 4). Density ellipses which enclose 90% of the points within each group show Channel mixing ratios enhanced compared to those of NNW. The enhancement of NO_3^- may be due to three possible reaction routes: (1) uptake of HNO_3 by sea salt, (2) uptake of HNO_3 by alkaline dust, primarily by reaction with $CaCO_3$, or (3) formation of fine mode NH_4NO_3. The first pathway may be eliminated since there is little difference in the availability of Na^+ between Channel and NNW (Figure 4). Further, several of the high NO_3^- samples (circles in Figure 4) appear at low concentrations of Na^+. Four of the high NO_3^- samples (blue circles in Figure 4) do have high Na^+ concentrations; however, these samples also have the highest nss-Ca^{2+} measured (Figure 4). This suggests the high Na^+ in these samples is due to crustal dust rather than to sea salt. All of the high NO_3^- samples are also high nss-Ca^{2+} samples. In addition to the high NO_3^- markers (circles), there are many samples with enhanced dust (red squares in Figure 4). These samples do not have enhanced HNO_3, which suggests that both HNO_3 and nss-Ca^{2+} need to be enhanced to yield enhanced NO_3^- via uptake on dust. Another possible explanation for the enhanced NO_3^- may be the formation of fine mode NH_4NO_3 rather than coarse mode uptake of NO_3^-. All of the enhanced NO_3^- samples are observed to have enhanced NH_4^+ as well (Figure 4). Most of the markers also show enhanced nss-$SO_4^=$ (Figure 4). Hence both mechanisms 2 and 3 may be important.

[18] Taking nss-Ca^{2+} values >100 neq/m^3 to indicate enhanced dust, there are clearly two populations of NO_3^- (Figure 5). Samples where NO_3^- is $\gtrsim$ about 100 neq/m^3 (circles in Figure 5) tend to fall near the 1:1 line, although generally there is excess nss-Ca^{2+} compared to NO_3^-. The other population is denoted by red squares. For these samples, although nss-Ca^{2+} indicates an abundance of dust, there is little appreciable increase in NO_3^-. Note that the one green square indicates a sample that is likely to be predominantly sea salt, since it lies on the seawater slope shown in Figure 3. The blue circles in Figure 5 have NO_3^- in excess of 100 neq/m^3, yet they are well away from the 1:1 line. Given their very high amount of nss-Ca^{2+}, it is possible that either the sample was obtained prior to the air mass reaching chemical equilibrium between the dust and HNO_3, or there was insufficient HNO_3 to produce more particulate NO_3^-. The correlation between the black circles and nss-Ca^{2+} is

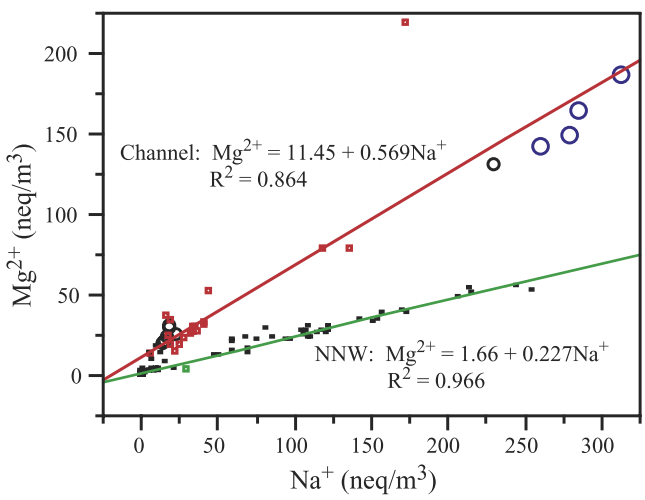

Figure 3. Mg^{2+} versus Na^+. Red linear fit to Channel data points; green fit to NNW data points. Circles indicate dust samples with enhanced NO_3^- and nss-$SO_4^=$. Red squares indicate dust samples without enhanced pollution species.

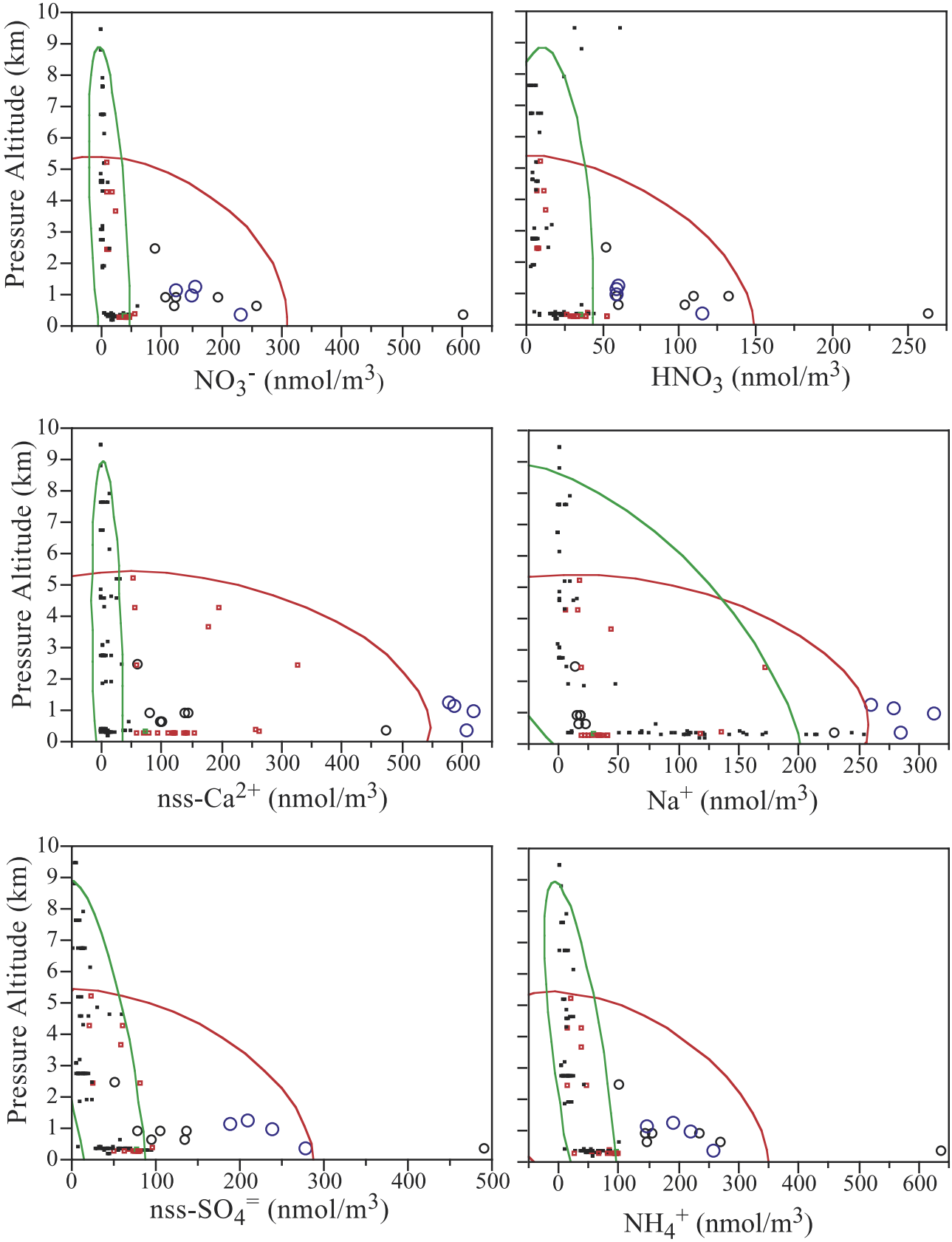

Figure 4. Aerosol and HNO_3 mixing ratios shown as a function of altitude. The density ellipses enclose 90% of the points within their respective groups, Channel (red ellipse) and NNW (green ellipse). Circles indicate dust samples with enhanced NO_3^- and nss-$SO_4^=$. Red squares indicate dust samples without enhanced pollution species.

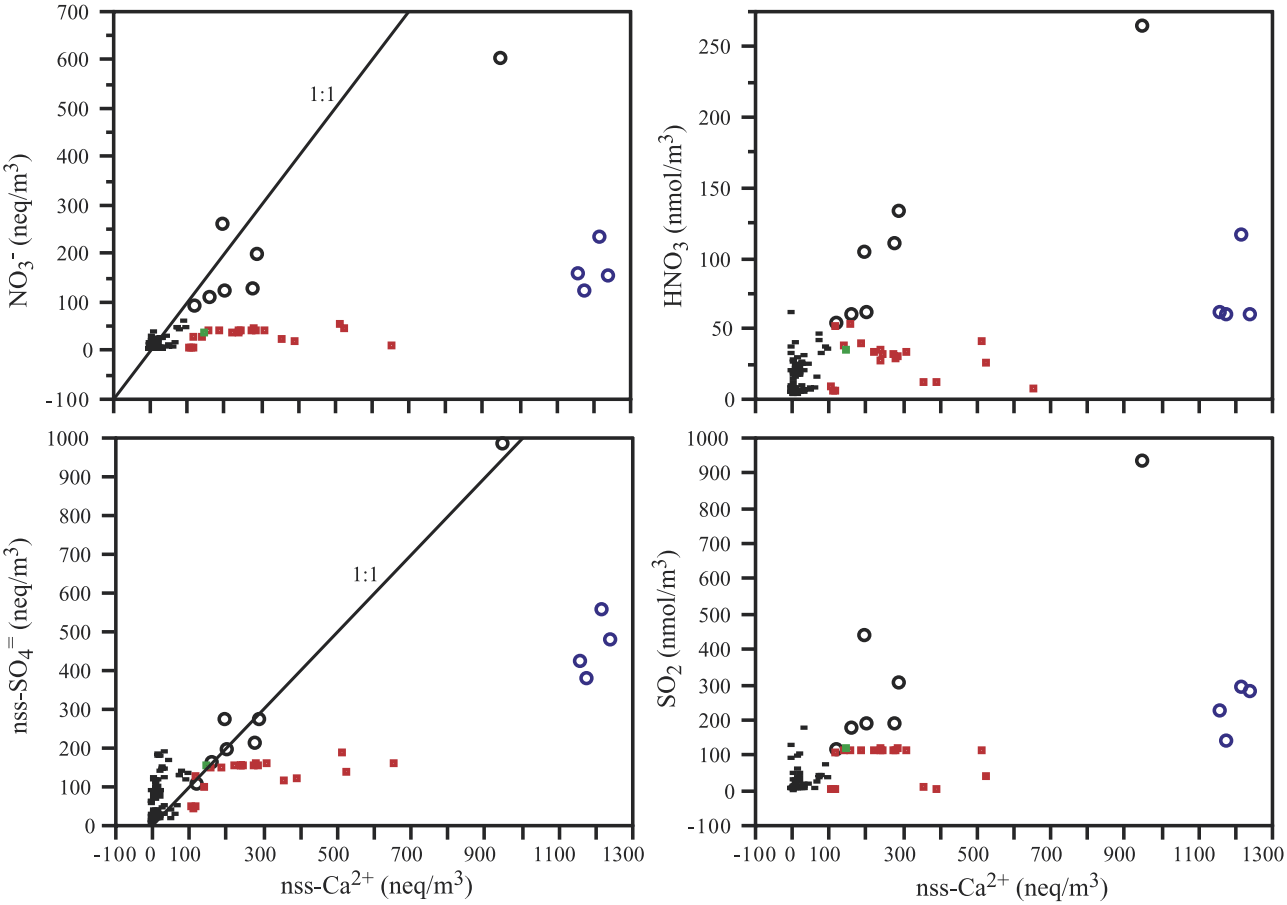

Figure 5. NO_3^-, nss-$SO_4^=$, HNO_3, and SO_2 shown as a function of dust (nss-Ca^{2+}). Circles indicate dust samples with enhanced NO_3^- and nss-$SO_4^=$. Red squares indicate dust samples without enhanced pollution species.

even closer to 1:1 for nss-$SO_4^=$ (Figure 5) than for NO_3^-. Again, there is little increase in nss-$SO_4^=$ with increasing nss-Ca^{2+} for the red square population. The blue circles are still set apart with respect to nss-$SO_4^=$ and nss-Ca^{2+}. HNO_3 and SO_2 (Figure 5), suggest the circles reflect the presence of higher levels of gas phase pollution than is present for the red squares (or the non-dust-enhanced black squares). This suggests that only dust intermingled with a sufficient amount of gas phase pollution will show significant uptake of NO_3^- and $SO_4^=$. Note that where nss-Ca^{2+} is low, there are still appreciable amounts of nss-$SO_4^=$. Presumably, this nss-$SO_4^=$ is due to uptake of nss-$SO_4^=$ on sea salts (coarse mode) or the presence of fine mode NH_4HSO_4 and $(NH_4)_2SO_4$. These results are similar to those reported by *Choi et al.* [2001]. They also reported cases in Seoul where some dust events were enhanced in pollution species, while other events were not.

[19] Next consider the possibility that the observed NO_3^- resides in fine mode NH_4NO_3 particles. There is a stunning correlation between NO_3^- and NH_4^+ (Figure 6), with the data points lying along the 1:1 line indicative of NH_4NO_3. There is some excess NH_4^+ compared to the NO_3^-, but not much. This suggests that particulate NO_3^- is in fine rather than coarse mode. However, the relationship between nss-$SO_4^=$ and NH_4^+ (Figure 6) argues against this scenario. There is clearly more than enough nss-$SO_4^=$ to accommodate all of the NH_4^+. Given the preferential formation of NH_4HSO_4 and $(NH_4)_2SO_4$ to that of the more volatile NH_4NO_3 for typical atmospheric temperatures and pressures, it seems unlikely that the bulk of NH_4^+ is associated with NO_3^- in this region. The correlation observed here may be coincidental. There are very good correlations between NH_4^+ and both HNO_3 and SO_2 (Figure 6) suggesting that NH_4^+ is simply a good tracer for pollutants. Investigating this possibility further, there are excellent correlations between CO and NH_4^+ (R^2 = 0.94) and Ethyne/CO and NH_4^+ (R^2 = 0.92) for the dust sector data (Figure 7). Both of these, CO and Ethyne/CO, are used as tracers for pollution. Neither one plays any role in the formation of NH_4^+, which supports the assertion that the good correlation between NH_4^+ and NO_3^- seen here is coincidental. Although modeling work by *Song and Carmichael* [2001a] suggests that NH_4NO_3 may form along the "lower courses of the Huang River" (which underlies the path of the dust flows), there is evidence suggesting that NO_3^- is associated with the coarse mode. *Wu and Okada* [1994] found coarse NO_3^- in all of their samples collected in Nagoya, Japan, including on the surface of dust particles during a Kosa event. Further, *Kim and Park* [2001] comparing samples during a dust storm and nondust periods in Seoul, Korea, found that the maximum concentration of NH_4^+ was in the fine mode (<2 μm diameter) under both conditions. Meanwhile, both $SO_4^=$ and NO_3^- were enhanced

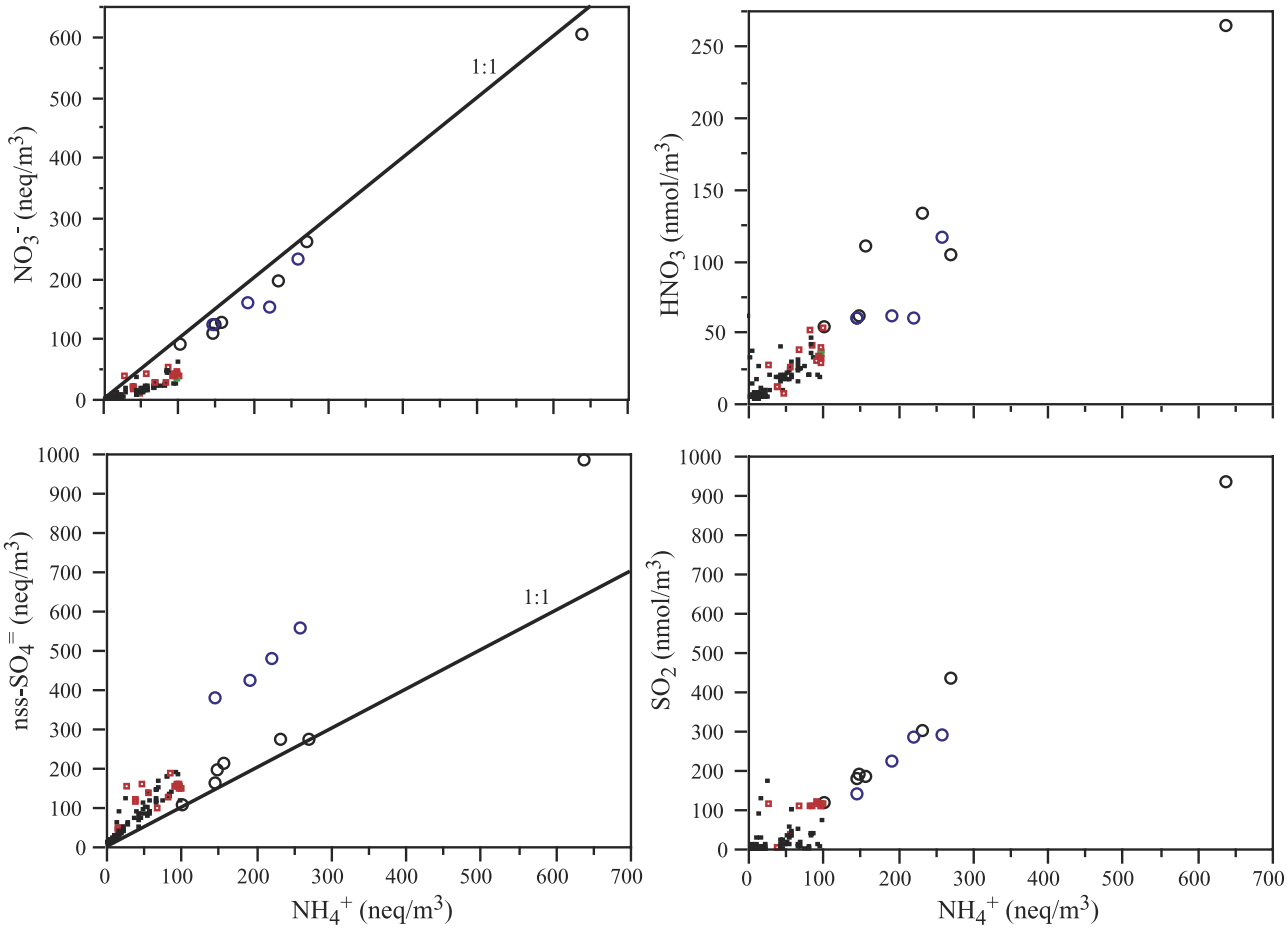

Figure 6. NO_3^-, nss-$SO_4^=$, HNO_3, and SO_2 shown as a function of NH_4^+. Circles indicate dust samples with enhanced NO_3^- and nss-$SO_4^=$. Red squares indicate dust samples without enhanced pollution species.

during the dust storm in the coarse fraction and were well correlated with coarse mode Ca^{2+}. In plots of *Kim and Park*'s [2001] size-resolved data, there is no evidence of a fine mode peak in NO_3^-. In the absence of size-resolved aerosol chemical measurements during TRACE-P, these observations argue against $SO_4^=$ and NO_3^- being primarily associated with NH_4^+ in the presence of dust.

[20] To estimate how much nss-$SO_4^=$ remains available for uptake on nss-Ca^{2+}, assume all particulate NH_4^+ is in the form of $(NH_4)_2SO_4$. Then, measured NH_4^+ equivalence is subtracted from measured nss-$SO_4^=$ equivalence to yield excess nss-$SO_4^=$ (Table 2). Further, NO_3^- is added to this excess nss-$SO_4^=$, and the sum is compared to nss-Ca^{2+} (Table 2). On average, 57% of the available nss-$SO_4^=$ can be taken up by NH_4^+, with the remainder available for uptake on dust and sea-salt surfaces. Even including NO_3^-, there is ample nss-Ca^{2+} to take up the measured NO_3^- and excess nss-$SO_4^=$. Indeed, even if there were no NH_4^+, the available nss-$SO_4^=$ and NO_3^- would only react with 76% of the available nss-Ca^{2+}.

[21] This suggests the uptake of nss-$SO_4^=$ and NO_3^-, in the heavily dust-impacted Channel samples, is limited by the amount of HNO_3 and SO_2 present, not by dust. Although, it is possible that all the available Ca^{2+} on the surface of the particles is associated with NO_3^- and $SO_4^=$, while the remaining Ca^{2+} is in the core of the particles where it cannot react with external gas phase species, this scenario is unlikely given the study by *Goodman et al.* [2000]. They found that in the presence of water vapor, the reaction of HNO_3 can proceed into the bulk of the particles driving off all of the $CO_3^=$. This makes all of the observed Ca^{2+} potentially available for reaction. Given this argument, the uptake observed during TRACE-P was probably limited by the availability of acidic gases, rather than dust.

[22] In comparison, in the NNW sector where dust is not so prevalent, there is insufficient nss-Ca^{2+} available to take up the available excess nss-$SO_4^=$ and NO_3^- (Table 2). Here these species are more likely to be associated with sea salt and are present at much lower levels than observed in the dust sector. To further illustrate this, Figure 8 shows excess nss-$SO_4^=$ versus nss-Ca^{2+}. If there was sufficient nss-$SO_4^=$ to react with all of the nss-Ca^{2+} present, the data would fall along the 1:1 line. In fact, where dust is not enhanced, there is more nss-$SO_4^=$ than can be accounted for by dust (black squares in Figure 8). This suggests this $SO_4^=$ is associated with fine mode NH_4^+ or perhaps with coarse mode sea salt. However, where there is plenty of dust (circles and red squares in Figure 8), excess nss-$SO_4^=$ is well correlated with nss-Ca^{2+} (R^2 = 0.87) with a slope of 0.2. Further, when NO_3^- is included in this analysis, the most polluted samples

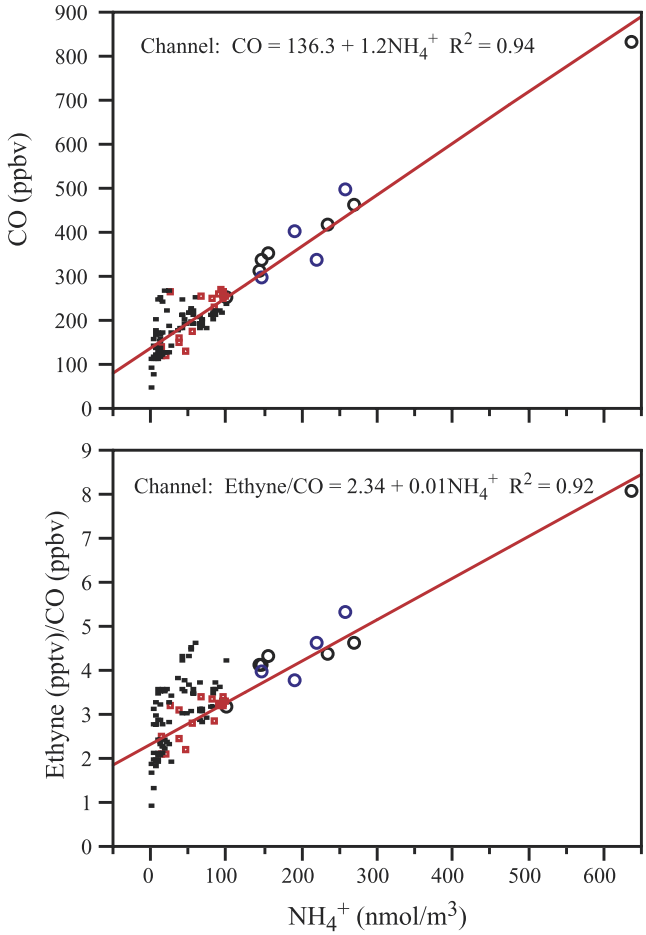

Figure 7. CO and Ethyne/CO versus $NH4^+$. All data from NNW and Channel are plotted, but only those from Channel are used for the linear fits. Circles indicate dust samples with enhanced NO_3^- and nss-$SO_4^=$. Red squares indicate dust samples without enhanced pollution species.

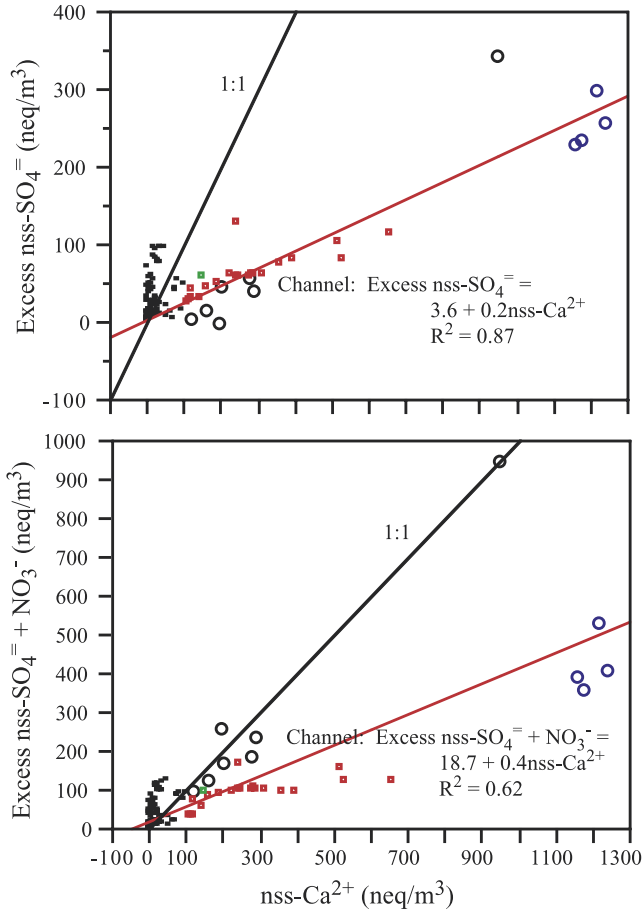

Figure 8. Excess nss-$SO_4^=$ and excess nss-$SO_4^=$ + NO_3^- versus nss-Ca^{2+} show how much of these species are available for uptake by dust after allowing NH_4^+ to take up as much nss-$SO_4^=$ as possible. Circles indicate dust samples with enhanced NO_3^- and nss-$SO_4^=$. Red squares indicate dust samples without enhanced pollution species.

are seen to lie along the 1:1 line (Figure 8), suggesting most of the $CO_3^=$ in the dust has been displaced. For the remainder of the dust enhanced samples, the uptake appears to be limited by the availability of HNO_3 and SO_2.

[23] This exercise probably underestimates the amount of excess nss-$SO_4^=$. As noted earlier, the non-sea-salt fractions have been underestimated, since some component of the Na^+ present is due to dust, even though it is all assumed to be sea salt. Thus the total amount of species in non-sea-salt fractions is somewhat higher than that shown here. Another issue to bear in mind comes from a study of individual particle composition. *Gao and Anderson* [2001] reported that fly ash particles (distinguishable from dust by their spherical rather than irregular shape) also show aggregation with $CaSO_4$. This is attributed to the use of $CaCO_3$ to scrub SO_2 from stack emissions. This can confound the interpre-

Table 2. Means, Standard Deviations, Medians, Minima, Maxima, and Number of Samples for Excess nss-$SO_4^=$ and NO_3^- Compared to Available Dust

	nss-$SO_4^=$, neq/m^3	NH_4^+, neq/m^3	Excess nss-$SO_4^=$, neq/m^3	NO_3^-, neq/m^3	Excess nss-$SO_4^=$ + NO_3^-, neq/m^3	nss-Ca^{2+}, neq/m^3
			Channel			
Mean ± st. dev.	182 ± 183	104 ± 115	78 ± 84	74 ± 110	152 ± 178	335 ± 353
Median (min.-max.)	156 (11–982)	92 (6–639)	58 (0–343)	40 (1–60)	103 (6–945)	229 (4–1245)
No. of samples	38	38	38	38	38	38
			NNW			
Mean ± st. dev.	70 ± 52	38 ± 29	32 ± 28	13 ± 16	45 ± 37	19 ± 24
Median (min.-max.)	62 (6–191)	26 (1–101)	23 (3–98)	6 (1–90)	39 (3–128)	12 (0–119)
No. of samples	77	77	77	77	77	74

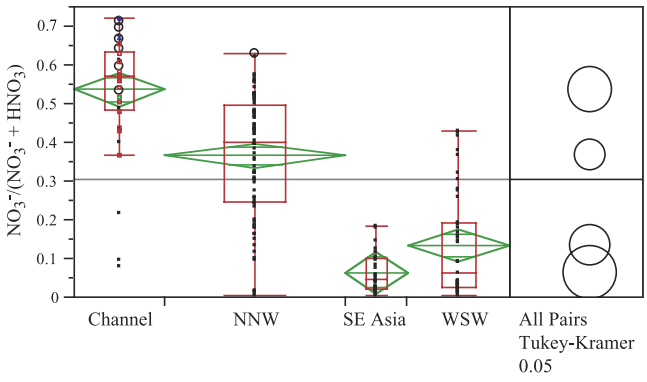

Figure 9. Comparison of NO_3^- partitioning between the dust sector (Channel), a sector with lots of sea salt (NNW), and two sectors where the influence of dust and sea salt are minimal (SE Asia and WSW). Green diamonds show means (center horizontal line) with the 95% confidence interval indicated by the upper and lower points of the diamonds, while the width of the diamond is proportional to the group size. Red rectangles show quantiles, with upper and lower bars indicating the 90th and 10th percentiles, respectively, top and bottom of box are at the 75th and 25th percentiles, respectively, and the red line in the box is the median. Circles on the right indicate whether the means are statistically different. The center of each circle is aligned with the mean of its respective group; the diameter of the circle spans the 95% confidence level. When the circles do not overlap, the means are significantly different. When they do overlap, the means may not be significantly different.

tation of non-size-resolved aerosol chemistry, because there will be a component of the nss-Ca^{2+} in the fine fraction which is not related to dust. However, in the presence of large dust outbreaks it is expected that this contribution to the total nss-Ca^{2+} will be small.

[24] Finally, the partitioning between particulate NO_3^- (p-NO_3^-) and gas phase HNO_3 is shown for dust (Channel) versus nondust (NNW) sectors (Figure 9). For comparison the partitioning is also shown for the other two sectors studied during TRACE-P, SE Asia and WSW. The samples from these sectors have minimal sea salt and dust influences (see *Jordan et al.* [2003] for a complete description of these sectors). Here we see that while the means for SE Asia and WSW may not be significantly different from each other, they are both significantly different from the other two, which are also significantly different from each other (Figure 9). For the groups least affected by the presence of sea salt and dust (SE Asia and WSW), the amount p-NO_3^- accounts for is only 6–13% of the total NO_3^- (t-NO_3^- = p-NO_3^- + HNO_3) present, on average (Table 3). Where dust is not a dominant component of the atmosphere (NNW), p-NO_3^- accounts for 37% of the t-NO_3^- on average, probably due to the influence of sea salts in this sector. For the dust sector, p-NO_3^- makes up 54% of the total on average, with maximum values of 72% observed (Table 3). These numbers agree well with those predicted by *Song and Carmichael* [2001a] where 10–50% of t-NO_3^- would be particulate in the presence of dust and sea salts, with >70% in dust and sea salt plume centers in the boundary layer, while in the free troposphere, 10–30% would be p-NO_3^- on sea salts and >50% in dust plume centers.

4. Summary

[25] Dust storms are prevalent in East Asia, with the dust being carried downwind along well-defined routes [*Sun et al.*, 2001]. This dust starts out with very little NO_3^- or $SO_4^=$ in the dust grains [*Nishikawa et al.*, 1991; and *Zhang and Iwasaka*, 1999]. However, in the presence of pollution, these dust particles can take up NO_3^- and $SO_4^=$, altering both the partitioning between particulate and gas phases of these species, as well as their size distributions in the atmosphere (especially, $SO_4^=$). During the TRACE-P mission, dust was found to be well confined to a particular sector emanating from Asia in good agreement with the routes described by *Sun et al.* [2001].

[26] This dust sector also contained the highest mixing ratios of pollutant species observed, with gas-phase HNO_3 2.7 times higher on average than in the adjacent nondust sector. Similarly, SO_2, CO, and the ratio of Ethyne/CO were 6.2, 1.5, and 1.1 times higher in the dust samples. Sea salt could not account for the enhancements in NO_3^- and $SO_4^=$ (factors of 5.7 and 2.6, respectively), since the mean mixing ratios of Na^+ in the dust and nondust regions were comparable (64 and 57 nmol/m^3, respectively). Although a good correlation between NO_3^- and NH_4^+ was observed, it appears that this was coincidental. As a tracer of anthropogenic species, NH_4^+ also exhibited excellent correlations with CO and the Ethyne/CO ratio (0.94 and 0.92, respectively). These species are not involved in any way with NH_4^+ formation. Prior observations in East Asia where size-resolved data was available did not show fine mode peaks of NO_3^- when dust was present. Further, calculations showed that there is ample nss-$SO_4^=$ to occupy the available NH_4^+ and still have enough left over to react with dust.

[27] During TRACE-P, the uptake of NO_3^- and $SO_4^=$ appeared to be limited by the availability of gas phase species. Where there is ample HNO_3 and SO_2 along with dust particles, the uptake of NO_3^- and $SO_4^=$ can be substantial and in some cases may entirely drive off the $CO_3^=$ in the dust aerosol. The partitioning between particulate and gas-phase NO_3^- shows 54% of the total NO_3^- (t-NO_3^-) in the dust sector is in particulate (p-NO_3^-) phase on average. In some samples, p-NO_3^- exceeded 70%. This is in good agreement with model predictions [*Song and Carmichael*, 2001a]. In the nondust sector, p-NO_3^- constituted 37% of t-NO_3^-, likely due to the heavy influence of sea salt. Two other sectors with little influence of dust or sea salt had p-NO_3^- contributing a small fraction to the total, <15%.

[28] These results provide evidence of in situ uptake of acidic gases on alkaline dust particles in support of model predictions and laboratory studies. This uptake may result in

Table 3. Means, Standard Deviations, Medians, Minima, Maxima, and Number of Samples for Nitrate Partition Comparison $NO_3^-/(NO_3^- + HNO_3)$

NNW	Channel	WSW	SE Asia
0.37 ± 0.16	0.54 ± 0.15	0.13 ± 0.13	0.06 ± 0.05
0.40 (0.00–0.63)	0.57 (0.08–0.72)	0.06 (0.00–0.43)	0.04 (0.00–0.18)
76	38	43	26

enhanced removal of nitrogen from the atmosphere, which may be important on regional scales. The presence of NO_3^- and $SO_4^=$ on coarse particles may lead to enhanced acid deposition along with its detrimental effects to terrestrial ecosystems than would be observed in regions without dust outbreaks. Enhanced deposition of NO_3^- to marine ecosystems may make more of this limiting nutrient available to the coastal biota. These effects may be magnified, if emissions of pollutant N and S increase with further industrialization in East Asia.

[29] **Acknowledgments.** The authors wish to thank the NASA Global Tropospheric Chemistry Program and the National Research Council for their support of this work.

References

Chameides, W. L., and A. W. Stelson, Aqueous phase chemical processes in deliquescent sea-salt aerosols: A mechanism that couples the atmospheric cycles of S and sea salt, *J. Geophys. Res.*, *97*, 20,565–20,580, 1992.

Choi, J. C., M. Lee, Y. Chun, J. Kim, and S. Oh, Chemical composition and source signature of spring aerosol in Seoul, Korea, *J. Geophys. Res.*, *106*, 18,067–18,074, 2001.

Dentener, F. J., G. R. Carmichael, Y. Zhang, J. Lelieveld, and P. J. Crutzen, Role of mineral aerosol as a reactive surface in the global troposphere, *J. Geophys. Res.*, *101*, 22,869–22,889, 1996.

Derbyshire, E., X. Meng, and R. A. Kemp, Provenance, transport and characteristics of modern aeolian dust in western Gansu Province, China, and interpretation of the Quaternary loess record, *J. Arid Environ.*, *39*, 497–516, 1998.

Dibb, J. E., R. W. Talbot, E. Scheuer, G. Seid, M. Avery, and H. Singh, Aerosol chemical composition in Asian continental outflow during Transport and Chemical Evolution over the Pacific, *J. Geophys. Res.*, *108*(D21), 8815, doi:10.1029/2002JD003111, in press, 2003.

Fuelberg, H. E., C. Kiley, J. R. Hannan, D. J. Westberg, M. A. Avery, and R. E. Newell, Meteorological conditions and transport pathways during the transport and chemical evolution over the Pacific experiment, *J. Geophys. Res.*, *108*(D20), 8782, doi:10.1029/2002JD003092, 2003.

Gao, Y., and J. R. Anderson, Characteristics of Chinese aerosols determined by individual particle analysis, *J. Geophys. Res.*, *106*, 18,037–18,045, 2001.

Goodman, A. L., G. M. Underwood, and V. H. Grassian, A laboratory study of the heterogeneous reaction of nitric acid on calcium carbonate particles, *J. Geophys. Res.*, *105*, 29,053–29,064, 2000.

Jordan, C. E., et al., Chemical and physical properties of bulk aerosols within four sectors observed during Transport and Chemical Evolution over the Pacific, *J. Geophys. Res.*, *108*(D21), 8813, doi:10.1029/2002JD003337, in press, 2003.

Keene, W. C., A. A. P. Pszenny, J. N. Galloway, and M. E. Hawley, Sea-salt corrections and interpretation of constituent ratios in marine precipitation, *J. Geophys. Res.*, *91*, 6647–6658, 1986.

Kim, B.-G., and S.-U. Park, Transport and evolution of a winter-time Yellow sand observed in Korea, *Atmos. Environ.*, *35*, 3191–3201, 2001.

Liu, T. S., *Loess and the Environment*, 251 pp., China Ocean, Beijing, 1985.

Minoura, H., S. Mizawa, and Y. Iwasaka, Seasonal changes in the concentrations of major cations and anions in precipitations in urban Nagoya, Japan: Local emission and long-range transport by Asian dust storms (KOSA) and typhoons, *J. Meteorol. Soc. Jpn.*, *76*, 13–27, 1998.

Nishikawa, M., S. Kanamori, N. Kanamori, and T. Misoguchi, Environmental significance of Kosa aerosol (yellow sand dust) collected in Japan, in *Proc. Second IUAPPA Reg. Conf. Air Pollut.*, pp. 35–41, Int. Union of Air Pollut. Prev. and Environ. Protect. Assoc., Brighton, UK, 1991.

Parungo, F., Y. Kim, C.-J. Zhu, J. Harris, R. Schnell, X.-S. Li, D.-Z. Yang, M.-Y. Zhou, Z. Chen, and K. Park, Asian dust storms and their effects on radiation and climate, *STC Rep. 2906*, Sci. and Tech. Corp., Hampton, Va., 1995.

Phadnis, M. J., and G. R. Carmichael, Influence of mineral aerosol on the tropospheric chemistry of East Asia, *J. Atmos. Chem.*, *36*, 285–323, 2000.

Pye, K., *Aeolian Dust and Dust Deposits*, Academic, San Diego, California, 1987.

Song, C. H., and G. R. Carmichael, A three-dimensional modeling investigation of the evolution processes of dust and sea-salt particles in East Asia, *J. Geophys. Res.*, *106*, 18,131–18,154, 2001a.

Song, C. H., and G. R. Carmichael, Gas-particle partitioning of nitric acid modulated by alkaline aerosol, *J. Atmos. Chem.*, *40*, 1–22, 2001b.

Sun, J., M. Zhang, and L. Tungsheng, Spatial and temporal characteristics of dust storms in China and its surrounding regions, 1960–1999: Relations to source area and climate, *J. Geophys. Res.*, *106*, 10,325–10,333, 2001.

Underwood, G. M., C. H. Song, M. Phadnis, G. R. Carmichael, and V. H. Grassian, Heterogeneous reactions of NO_2 and HNO_3 on oxides and mineral dust: A combined laboratory and modeling study, *J. Geophys. Res.*, *106*, 18,055–18,066, 2001.

Wilson, T. R. S., Salinity and the major elements of sea water, in *Chemical Oceanography*, vol. 1, 2nd ed., edited by J. P. Riley and G. Skirrow, pp. 365–413, Academic, San Diego, Calif., 1975.

Wu, P.-M., and K. Okada, Nature of coarse nitrate particles in the atmosphere—A single particle approach, *Atmos. Environ.*, *28*, 2053–2060, 1994.

Xiao, H., G. R. Carmichael, J. Durchenwald, D. Thornton, and A. Bandy, Long-range transport of SO_x and dust in East Asia during the PEM B experiment, *J. Geophys. Res.*, *102*, 28,589–28,612, 1997.

Zhang, D., and Y. Iwasaka, Nitrate and sulfate in individual Asian dust-storm particles in Beijing, China in spring of 1995 and 1996, *Atmos. Environ.*, *33*, 3213–3223, 1999.

Zhang, Y., Y. Sunwoo, V. Kotamarthi, and G. Carmichael, Photochemical oxidant processes in the presence of dust: An evaluation of the impact of dust on particulate nitrate and ozone formation, *J. Appl. Meteorol.*, *33*, 813–824, 1994.

B. E. Anderson and C. E. Jordan, NASA Langley Research Center, MS 483, Hampton, VA 23681, USA. (b.e.anderson@larc.nasa.gov; c.e.jordan@larc.nasa.gov)

J. E. Dibb, Climate Change Research Center, Institute for the Study of Earth, Oceans, and Space, University of New Hampshire, Durham, NH 03824, USA. (jack.dibb@unh.edu)

H. E. Fuelberg, Department of Meteorology, Florida State University, Tallahassee, FL 32306, USA. (Fuelberg@met.fsu.edu)